# Homogeneous and evanescent contributions in scalar near-field diffraction

Marek W. Kowarz

The contributions of homogeneous and evanescent waves to two-dimensional near-field diffraction patterns of scalar optical fields are examined in detail. The total plane-integrated intensities of the two contributions are introduced as convenient measures of their relative importance. As an example, the diffraction of a plane wave by a slit is considered.

*Key words:* Diffraction, near field, Fourier optics.

## 1. Introduction

Important recent developments in near-field microscopy, near-field spectroscopy, and high-density optical data storage have prompted considerable interest in near-field optics,[1–4] in which both the spatial features of the objects and the propagation distances can be much smaller than a wavelength. Unlike conventional optical systems, whose resolution is fundamentally limited by the wavelength, near-field systems can achieve subwavelength resolution by interaction with the evanescent near field, which carries information about spatial periods in the structure of an object that are smaller than a wavelength (see Fig. 1).

In this paper we elucidate the effects of diffraction in the near field by examining the separate contributions of homogeneous and evanescent (inhomogeneous) waves to two-dimensional (2-D) near-field diffraction patterns of scalar fields. Some discussion of near-field diffraction based on such a decomposition can also be found in papers by Harvey[5] and by Massey.[6] The consequences of neglecting evanescent waves in certain near-field distributions have been discussed by Carter.[7,8] For the sake of mathematical simplicity, and also because in the 2-D case the exact electromagnetic diffraction problem can be described by a scalar theory,[9] we restrict our analysis to 2-D diffraction.

First, in Section 2 some basic relations for calculating the homogeneous and the evanescent contributions to an arbitrary field are discussed. Then in Section 3 the concepts of total homogeneous intensity and total evanescent intensity are introduced. Finally, in Section 4 the behavior of the two contributions is illustrated for the case when a plane wave is diffracted by a slit in an opaque screen.

## 2. Homogeneous and Evanescent Contributions

Let us consider a 2-D monochromatic scalar optical field $V(x, z, t) = U(x, z)\exp(-i\omega t)$ ($\omega$ being the temporal frequency). $U(x, z)$ obeys the 2-D Helmholtz equation,

$$(\nabla^2 + k^2)U(x, z) = 0, \tag{2.1}$$

where $\nabla^2 \equiv \partial^2/\partial x^2 + \partial^2/\partial z^2$, $k = \omega/c = 2\pi/\lambda$ is the free-space wave number, $c$ is the speed of light in vacuum, and $\lambda$ is the wavelength.

We are interested in free-space propagation of the field $U(x, z)$ from the plane $z = 0$ into the half-space $z > 0$. We shall assume that all sources, scatterers, diffracting apertures, etc., are located in the half-space $z < 0$. Using the angular spectrum representation,[10–15] we can write the field $U(x, z)$ for $z \geq 0$ as the sum of a homogeneous contribution $U_h(x, z)$ and an evanescent (inhomogeneous) contribution $U_i(x, z)$,

$$U(x, z) = U_h(x, z) + U_i(x, z). \tag{2.2}$$

$U_h(x, z)$ is a superposition of homogeneous plane waves that propagate into the half-space $z > 0$,

$$U_h(x, z) = \int_{|u_x| \leq 1} a(u_x)\exp(iku_x x)\exp[ikz(1 - u_x^2)^{1/2}]\mathrm{d}u_x, \tag{2.3a}$$

The author is with the Institute of Optics, University of Rochester, Rochester, New York 14627.

Received 14 July 1994; revised manuscript received 3 January 1995.

0003-6935/95/173055-09$06.00/0.

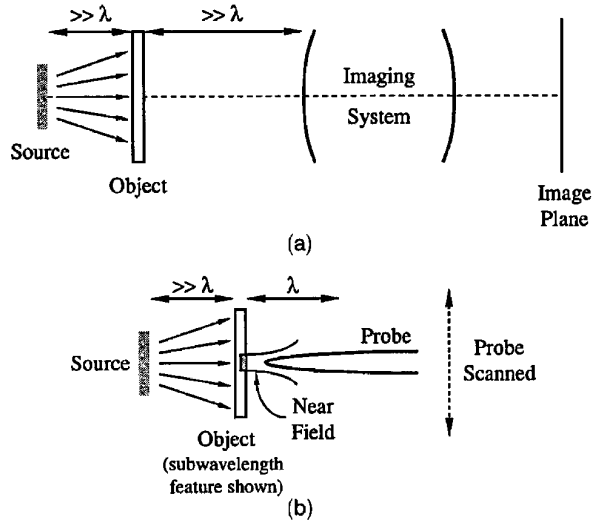


Fig. 1. Diagrams of (a) a conventional optical microscope and (b) a collection-mode near-field scanning optical microscope.

whereas $U_i(x, z)$ is a superposition of evanescent (inhomogeneous) plane waves that decay exponentially along the positive $z$ direction,

$$U_i(x, z) = \int_{|u_x|>1} a(u_x)\exp(iku_x x)\exp[-kz(u_x^2 - 1)^{1/2}]\mathrm{d}u_x. \tag{2.3b}$$

It should be noted that the homogeneous and the evanescent contributions each separately satisfy the Helmholtz equation.

The spectral amplitude function $a(u_x)$ appearing in Eqs. (2.3) is the spatial Fourier transform of the field distribution $U(x, 0)$ in the plane $z = 0$:

$$a(u_x) = \frac{k}{2\pi}\int_{-\infty}^{\infty} U(x', 0)\exp(-iku_x x')\mathrm{d}x'. \tag{2.4}$$

For the near-field geometries of interest in this paper we can restrict our analysis to well-behaved functions $U(x, 0)$ that are of finite support, i.e., well-behaved functions that vanish outside some finite $x$ range. $U(x, 0)$ is then square integrable; furthermore, $a(u_x)$ is the boundary value on the real $u_x$ axis of an entire analytic function.[16]

Using relation (2.4), we may rewrite Eqs. (2.3) as

$$U_h(x, z) = \int_{-\infty}^{\infty} \mathcal{H}_h(x - x', z)U(x', 0)\mathrm{d}x', \tag{2.5a}$$

$$U_i(x, z) = \int_{-\infty}^{\infty} \mathcal{H}_i(x - x', z)U(x', 0)\mathrm{d}x', \tag{2.5b}$$

with the kernels $\mathcal{H}_h(x, z)$ and $\mathcal{H}_i(x, z)$ given by the formulas

$$\mathcal{H}_h(x, z) \equiv \frac{k}{\pi}\int_0^1 \cos(ku_x x)\exp[ikz(1 - u_x^2)^{1/2}]\mathrm{d}u_x \tag{2.6a}$$

$$\mathcal{H}_i(x, z) \equiv \frac{k}{\pi}\int_1^{\infty} \cos(ku_x x)\exp[-kz(u_x^2 - 1)^{1/2}]\mathrm{d}u_x. \tag{2.6b}$$

It can readily be shown that

$$\mathcal{H}(x, z) \equiv \mathcal{H}_h(x, z) + \mathcal{H}_i(x, z) = \frac{ikz}{2(x^2 + z^2)^{1/2}} H_1^{(1)}[k(x^2 + z^2)^{1/2}], \tag{2.7}$$

where $H_1^{(1)}$ is a Hankel function of the first kind and first order. Expression (2.7) is the usual 2-D free-space wave propagator.[17]

If we let $z = 0$ in Eqs. (2.6), the integrations with respect to $u_x$ can be performed at once, yielding

$$\mathcal{H}_h(x, 0) = \frac{1}{\pi}\frac{\sin(kx)}{x}, \tag{2.8a}$$

$$\mathcal{H}_i(x, 0) = \delta(x) - \frac{1}{\pi}\frac{\sin(kx)}{x}, \tag{2.8b}$$

where $\delta(x)$ is the Dirac delta function. After substituting these relations into Eqs. (2.5), we find that

$$U_h(x, 0) = \frac{1}{\pi}\int_{-\infty}^{\infty} \frac{\sin[k(x - x')]}{(x - x')} U(x', 0)\mathrm{d}x', \tag{2.9a}$$

$$U_i(x, 0) = U(x, 0) - \frac{1}{\pi}\int_{-\infty}^{\infty} \frac{\sin[k(x - x')]}{(x - x')} U(x', 0)\mathrm{d}x'. \tag{2.9b}$$

Because the location of the plane $z = 0$ is essentially arbitrary, analogous expressions must also apply to

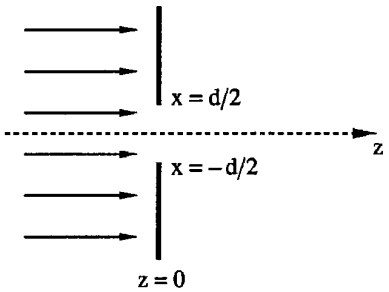


Fig. 2. Slit of width $d$ in an opaque screen, illuminated by a normally incident plane wave.

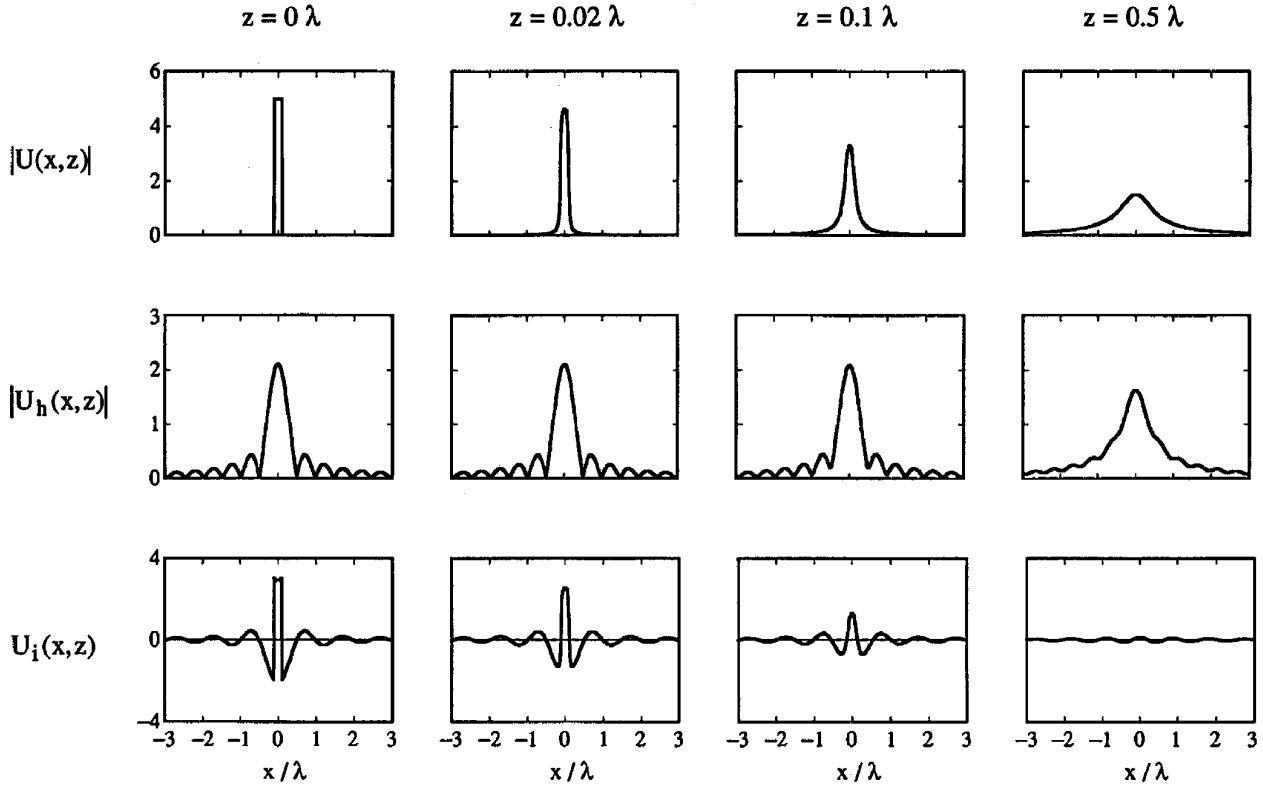


Fig. 3. Near-field diffraction patterns showing $|U(x, z)|$, $|U_h(x, z)|$, and $U_i(x, z)$ for a slit of width $d = 0.2\lambda$ with the choice $K = \lambda/d = 5$.

any plane $z = \text{const.} \geq 0$:

$$U_h(x, z) = \frac{1}{\pi}\int_{-\infty}^{\infty} \frac{\sin[k(x - x')]}{(x - x')}\, U(x', z)\mathrm{d}x', \tag{2.10a}$$

$$U_i(x, z) = U(x, z) - \frac{1}{\pi}\int_{-\infty}^{\infty} \frac{\sin[k(x - x')]}{(x - x')}\, U(x', z)\mathrm{d}x'. \tag{2.10b}$$

We see from the preceding discussion that there are three alternative pairs of expressions that can be used to determine the homogeneous and the evanescent contributions to the field in any plane $z = \text{const.} \geq 0$: Eqs. (2.3), Eqs. (2.5), and Eqs. (2.10). The first pair, Eqs. (2.3), expresses $U_h(x, z)$ and $U_i(x, z)$ in terms of the spectral amplitude function, $a(u_x)$, which itself can be computed by taking a Fourier transform of the field distribution $U(x, 0)$ in the plane $z = 0$ [see Eq. (2.4)]. In the near field these equations are well suited for numerical implementation because all the integrations can be performed with fast Fourier transforms.

The second pair of equations, Eqs. (2.5), determines $U_h(x, z)$ and $U_i(x, z)$ directly from the field distribution $U(x, 0)$ in the plane $z = 0$. However, for arbitrary $z$ the kernels $\mathcal{H}_h(x, z)$ and $\mathcal{H}_i(x, z)$, given by Eqs. (2.6), cannot readily be expressed in closed form.

Last, Eqs. (2.10) can be used to obtain $U_h(x, z)$ and $U_i(x, z)$ in any plane $z = \text{const.} \geq 0$ from knowledge of the field distribution $U(x, z)$ in that plane. If $U(x, z)$ is not known, but either $U_h(x, z)$ or $U_i(x, z)$ is known, Eqs. (2.10a) and (2.10b) are of the form of Fredholm integral equations of the first and the second kind, respectively, for the unknown $U(x, z)$. The integral operator that appears in Eq. (2.10a) has been studied extensively and occurs in a variety of contexts.[18–21]

### 3. Total Intensities

We shall now introduce the concepts of total (plane-integrated) homogeneous intensity and total (plane-integrated) evanescent intensity as rough convenient measures of the relative importance of the contributions $U_h(x, z)$ and $U_i(x, z)$ to the field distribution $U(x, z)$.

Using Eq. (2.2), we can write the intensity of the field $I(x, z) \equiv |U(x, z)|^2$ in the form

$$I(x, z) = I_h(x, z) + I_i(x, z) + I_{hi}(x, z), \tag{3.1}$$

where

$$I_h(x, z) \equiv |U_h(x, z)|^2, \tag{3.2a}$$

$$I_i(x, z) \equiv |U_i(x, z)|^2, \tag{3.2b}$$

are the intensities of the homogeneous and of the evanescent contributions, respectively, and the term

$$I_{hi}(x, z) \equiv U_h^*(x, z)U_i(x, z) + U_h(x, z)U_i^*(x, z) \tag{3.2c}$$

arises from interference between the homogeneous and the evanescent contributions. We now define

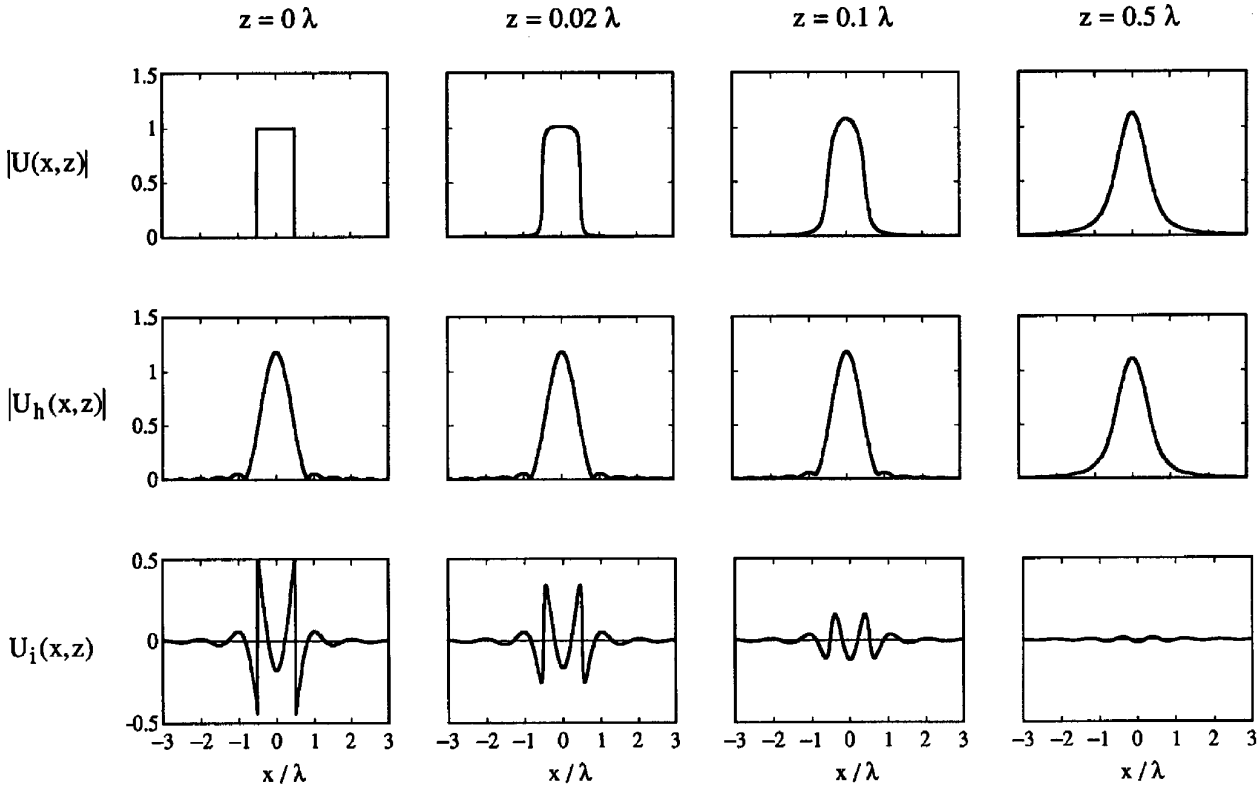


Fig. 4. Same as Fig. 3 but for width $d = 1\lambda$ and $K = \lambda/d = 1$.

the total intensity $I_{\text{tot}}(z)$, the total homogeneous intensity $I_{\text{tot}}^{(h)}(z)$, and the total evanescent (inhomogeneous) intensity $I_{\text{tot}}^{(i)}(z)$ by the expressions

$$I_{\text{tot}}(z) \equiv \int_{-\infty}^{\infty} I(x, z)\mathrm{d}x, \tag{3.3}$$

$$I_{\text{tot}}^{(h)}(z) \equiv \int_{-\infty}^{\infty} I_h(x, z)\mathrm{d}x, \tag{3.4a}$$

$$I_{\text{tot}}^{(i)}(z) \equiv \int_{-\infty}^{\infty} I_i(x, z)\mathrm{d}x, \tag{3.4b}$$

respectively.

From Eqs. (2.3) and (3.1)–(3.4) it follows that the total intensity is just the sum

$$I_{\text{tot}}(z) = I_{\text{tot}}^{(h)}(z) + I_{\text{tot}}^{(i)}(z), \tag{3.5}$$

where

$$I_{\text{tot}}^{(h)}(z) = \frac{2\pi}{k}\int_{|u_x|\le 1} |a(u_x)|^2 \mathrm{d}u_x, \tag{3.6a}$$

$$I_{\text{tot}}^{(i)}(z) = \frac{2\pi}{k}\int_{|u_x|>1} |a(u_x)|^2 \exp[-2kz(u_x^2 - 1)^{1/2}]\mathrm{d}u_x. \tag{3.6b}$$

There are only two terms in Eq. (3.5) because the integrated interference term can be shown to be identically zero. Furthermore, as is evident from Eq. (3.6a), the total homogeneous intensity is conserved on propagation in the sense that $I_{\text{tot}}^{(h)}(z)$ is independent of $z$. Hence we may drop the $z$ argument in $I_{\text{tot}}^{(h)}(z)$, and we will do so from now on. The conservation of total homogeneous intensity on propagation and related conservation laws is discussed in Refs. 22–25.

By substituting the spectral amplitude function from Eq. (2.4) into Eqs. (3.6), we can rewrite the total intensities $I_{\text{tot}}^{(h)}$ and $I_{\text{tot}}^{(i)}(z)$ in terms of the field distribution $U(x, 0)$ in the plane $z = 0$ as

$$I_{\text{tot}}^{(h)} = \frac{1}{\pi}\int_{-\infty}^{\infty}\mathrm{d}x' \int_{-\infty}^{\infty}\mathrm{d}x'' \frac{\sin[k(x' - x'')]}{(x' - x'')} \times U^*(x', 0)U(x'', 0), \tag{3.7a}$$

$$I_{\text{tot}}^{(i)}(z) = \int_{-\infty}^{\infty}\mathrm{d}x' \int_{-\infty}^{\infty}\mathrm{d}x''\, \mathcal{H}_i(x' - x'', 2z)U^*(x', 0)U(x'', 0), \tag{3.7b}$$

where the kernel $\mathcal{H}_i(x, z)$ is given by Eq. (2.6b). Alternatively, using the fact that $I_{\text{tot}}^{(h)}$ is independent of $z$, we can also express $I_{\text{tot}}^{(h)}$ and $I_{\text{tot}}^{(i)}(z)$ in terms of the field distribution $U(x, z)$ in an arbitrary plane $z =$

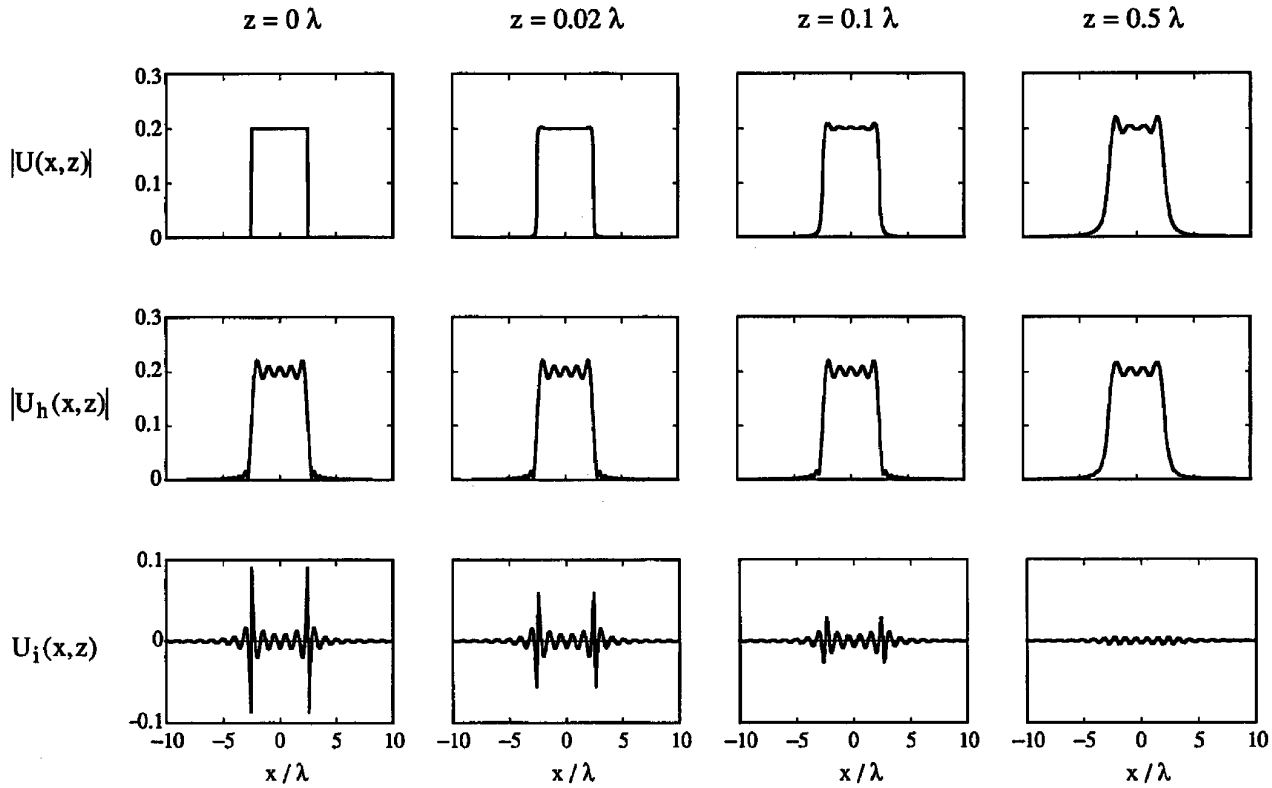


Fig. 5. Same as Fig. 3 but for width $d = 5\lambda$ and $K = \lambda/d = 0.2$.

const. $\geq 0$, as follows:

$$I_{\text{tot}}^{(h)} = \frac{1}{\pi}\int_{-\infty}^{\infty} dx' \int_{-\infty}^{\infty} dx'' \frac{\sin[k(x' - x'')]}{(x' - x'')} \times U^*(x', z)U(x'', z), \tag{3.8a}$$

$$I_{\text{tot}}^{(i)}(z) = \int_{-\infty}^{\infty} |U(x, z)|^2 dx - \frac{1}{\pi}\int_{-\infty}^{\infty} dx' \int_{-\infty}^{\infty} dx'' \times \frac{\sin[k(x' - x'')]}{(x' - x'')} U^*(x', z)U(x'', z). \tag{3.8b}$$

Evidently the total intensities $I_{\text{tot}}(z)$, $I_{\text{tot}}^{(h)}$, and $I_{\text{tot}}^{(i)}(z)$ are useful only if they are finite quantities. In this connection it should be pointed out that there are physically realistic field distributions that have infinite total intensity but finite total energy flux.[26] Because the field distribution $U(x, 0)$ that we are considering is square integrable [see remarks below Eq. (2.4)], $I_{\text{tot}}(0)$ is finite, and, consequently, so are $I_{\text{tot}}(z)$, $I_{\text{tot}}^{(h)}$, and $I_{\text{tot}}^{(i)}(z)$ because, as can easily be shown,

$$I_{\text{tot}}(z) \leq I_{\text{tot}}(0),\ I_{\text{tot}}^{(h)} < I_{\text{tot}}(0), \quad I_{\text{tot}}^{(i)}(z) < I_{\text{tot}}(0).$$

Instead of using the total intensities $I_{\text{tot}}^{(h)}$ and $I_{\text{tot}}^{(i)}(z)$ as measures of the relative importance of $U_h(x, z)$ and $U_i(x, z)$, one might consider using the total energy flux $F_{\text{tot}}^{(h)}$ and the total reactive energy $F_{\text{tot}}^{(i)}(z)$ for this purpose. As discussed in Appendix A, these quantities can be defined by means of the scalar analog of the complex Poynting theorem. In terms of the spectral amplitude function $a(u_x)$, they may be written as

$$F_{\text{tot}}^{(h)} = 4\pi\omega\alpha \int_{|u_x|\leq 1} (1 - u_x^2)^{1/2} |a(u_x)|^2 du_x, \tag{3.9a}$$

$$F_{\text{tot}}^{(i)}(z) = 4\pi\omega\alpha \int_{|u_x|>1} (u_x^2 - 1)^{1/2} |a(u_x)|^2 \times \exp[-2kz(u_x^2 - 1)^{1/2}] du_x, \tag{3.9b}$$

$\alpha$ being a positive constant, as we demonstrate in Appendix A. Equations (3.9a) and (3.9b) should be compared with their counterparts for the total intensities, Eqs. (3.6a) and (3.6b). As expected, we see that the total energy flux $F_{\text{tot}}^{(h)}$ depends only upon the homogeneous contribution $U_h(x, z)$ and is independent of the propagation distance $z$, whereas the total reactive energy $F_{\text{tot}}^{(i)}(z)$ depends only upon the evanescent contribution $U_i(x, z)$ and decays with $z$. However, because of the multiplicative factor $(u_x^2 - 1)^{1/2}$ in Eq. (3.9b), the total reactive energy can diverge in cases when the total evanescent intensity is finite. In fact, for the example considered in Section 4 one can show that the total reactive energy does indeed diverge in the plane $z = 0$. For this reason we choose to use the total intensities $I_{\text{tot}}^{(h)}$ and $I_{\text{tot}}^{(i)}(z)$ rather than $F_{\text{tot}}^{(h)}$ and $F_{\text{tot}}^{(i)}(z)$ in our near-field analysis.

## 4. Diffraction by a Slit

The analysis of diffraction of light by an aperture in an opaque screen can be separated into the treatment of two distinct problems: the boundary-value problem and the propagation problem. The boundary-value problem consists of determining the field immediately behind the screen for a given incident field and known material properties of the screen, whereas the propagation problem involves determining the field at some distance from the screen when the field immediately behind the screen is known. Because in most cases it is very difficult to determine the exact boundary value of the field, approximate boundary conditions are often used, such as those given by the Rayleigh–Sommerfeld theories or the Kirchhoff theory.[27,28]

We now consider, as an example, the near-field diffraction of a plane wave normally incident upon a slit of width $d$ in an opaque screen (see Fig. 2), using approximate boundary conditions. We assume that directly behind the slit, in the plane $z = 0$, the field may be approximated by the Rayleigh–Sommerfeld boundary condition of the first kind[27,28]:

$$U(x, 0) = \begin{cases} U_{\text{inc}}(x, 0) & \text{for } -d/2 \le x \le d/2 \\ 0 & \text{otherwise} \end{cases}, \quad (4.1)$$

where $U_{\text{inc}}(x, z)$ represents the incident field. For the case of a normally incident plane wave, $U_{\text{inc}}(x, 0) = K$, where $K$ is a constant. It should be pointed out that, for the small slit widths of interest here, one would expect the actual field distribution in the plane $z = 0$, i.e., the solution to the rigorous boundary-value problem, to be rather different from the field distribution given by the above boundary condition. Nevertheless, we can still gain some understanding of propagation in the near field by employing this approximate boundary condition.

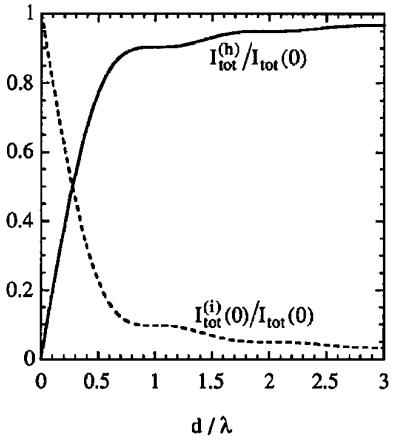


Fig. 6. Total homogeneous intensity $I^{(h)}_{\text{tot}}$ (which is independent of $z$) and total evanescent intensity $I^{(i)}_{\text{tot}}(0)$ in the plane $z = 0$ as functions of the slit width $d$. These curves were computed from Eqs. (4.5) and (4.8).

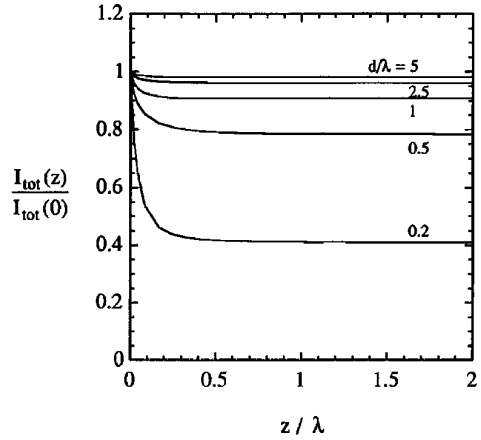


Fig. 7. Total intensity $I_{\text{tot}}(z) = I^{(h)}_{\text{tot}} + I^{(i)}_{\text{tot}}(z)$ computed from Eqs. (4.4b) and (4.5) as a function of the distance $z$ for various slit widths.

Using Eq. (2.4), we find that the spectral amplitude function associated with boundary condition (4.1) is

$$a(u_x) = \frac{K}{\pi} \frac{\sin(u_x k d/2)}{u_x}. \quad (4.2)$$

Consequently, according to Eqs. (2.3) and (3.6), the homogeneous and the evanescent contributions in any plane $z = \text{const.} \ge 0$ are

$$U_h(x, z) = \frac{K}{\pi} \int_{|u_x| \le 1} \frac{\sin(u_x k d/2)}{u_x} \exp(iku_x x) \times \exp[ikz(1 - u_x^2)^{1/2}] du_x, \quad (4.3a)$$

$$U_i(x, z) = \frac{K}{\pi} \int_{|u_x| > 1} \frac{\sin(u_x k d/2)}{u_x} \exp(iku_x x) \times \exp[-kz(u_x^2 - 1)^{1/2}] du_x, \quad (4.3b)$$

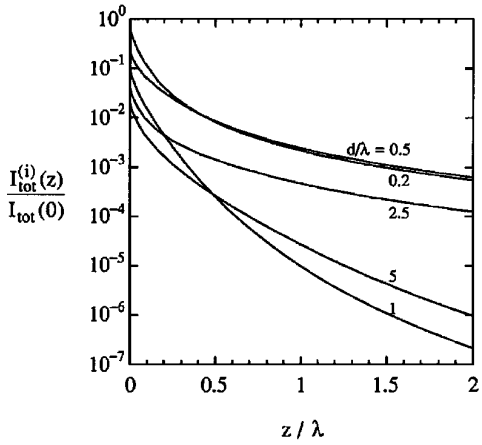


Fig. 8. Total evanescent intensity $I^{(i)}_{\text{tot}}(z)$ computed from Eq. (4.4b) as a function of the distance $z$ for various slit widths.

and the total intensities are

$$I_{\mathrm{tot}}^{(h)} = \frac{4I_{\mathrm{tot}}(0)}{\pi kd}\int_0^1 \frac{\sin^2(u_x kd/2)}{u_x^2}\,\mathrm{d}u_x, \qquad (4.4a)$$

$$I_{\mathrm{tot}}^{(i)}(z) = \frac{4I_{\mathrm{tot}}(0)}{\pi kd}\int_1^\infty \frac{\sin^2(u_x kd/2)}{u_x^2} \times \exp[-2kz(u_x^2-1)^{1/2}]\mathrm{d}u_x. \qquad (4.4b)$$

Here $I_{\mathrm{tot}}(0) = |K|^2 d$ is the total intensity in the plane $z = 0$. Equation (4.4a) for the total homogeneous intensity can be rewritten in a more compact form as

$$I_{\mathrm{tot}}^{(h)} = I_{\mathrm{tot}}(0)\left[\frac{2}{\pi}\,\mathrm{Si}(kd) - \frac{4}{\pi kd}\sin^2(kd/2)\right], \qquad (4.5)$$

where $\mathrm{Si}(\beta)$ is the sine integral

$$\mathrm{Si}(\beta) \equiv \int_0^\beta \frac{\sin t}{t}\,\mathrm{d}t. \qquad (4.6)$$

Furthermore, in the plane $z = 0$, expressions (4.3a) and (4.3b) for the homogeneous and the evanescent contributions reduce to

$$U_h(x,0) = \frac{K}{\pi}\{\mathrm{Si}[k(x+d/2)] - \mathrm{Si}[k(x-d/2)]\}, \qquad (4.7a)$$

$$U_i(x,0) = \begin{cases} \dfrac{K}{\pi}\{\pi - \mathrm{Si}[k(x+d/2)] + \mathrm{Si}[k(x-d/2)]\} & \text{for } -d/2 \le x \le d/2 \\ -\dfrac{K}{\pi}\{\mathrm{Si}[k(x+d/2)] - \mathrm{Si}[k(x-d/2)]\} & \text{otherwise} \end{cases}, \qquad (4.7b)$$

and expression (4.4b) for the total evanescent intensity reduces to

$$I_{\mathrm{tot}}^{(i)}(0) = I_{\mathrm{tot}}(0)\left[1 - \frac{2}{\pi}\,\mathrm{Si}(kd) + \frac{4}{\pi kd}\sin^2(kd/2)\right]. \qquad (4.8)$$

We can now examine the field $U(x, z)$, the homogeneous contribution $U_h(x, z)$, the evanescent contribution $U_i(x, z)$, the total intensity $I_{\mathrm{tot}}(z)$, the total homogeneous intensity $I_{\mathrm{tot}}^{(h)}$, and the total evanescent intensity $I_{\mathrm{tot}}^{(i)}(z)$ in the near field for specific values of the slit width $d$ and of the propagation distance $z$.

Figures 3–5 depict $|U(x, z)|$, $|U_h(x, z)|$, and $U_i(x, z)$ for $z = 0$, $z = 0.02\lambda$, $z = 0.1\lambda$, and $z = 0.5\lambda$. These figures were computed from Eqs. (4.3) with fast Fourier transforms. Figures 3, 4, and 5 pertain to slits of width $d = 0.2\lambda$, $d = 1\lambda$, and $d = 5\lambda$, respectively. We see that, for $z \ll \lambda$, changes in the field $U(x, z)$ from its initial value $U(x, 0)$ are mostly caused by the decay of the evanescent contribution $U_i(x, z)$ with only slight modifications in the homogeneous contribution $U_h(x, z)$. The decay of the evanescent contribution $U_i(x, z)$ is obviously most important for the case $d = 0.2\lambda$, and, consequently, for this slit width there is a substantial broadening and decrease in the amplitude of the field distribution $U(x, z)$ on propagation from the plane $z = 0$ to $z = 0.5\lambda$.

Figures 6–8 show $I_{\mathrm{tot}}^{(h)}$ and $I_{\mathrm{tot}}^{(i)}(0)$ as functions of the slit width $d$ and $I_{\mathrm{tot}}(z)$ and $I_{\mathrm{tot}}^{(i)}(z)$ as functions of the propagation distance $z$. From Fig. 6 we see that, for slit widths smaller than about half a wavelength, the total evanescent intensity $I_{\mathrm{tot}}^{(i)}(0)$ in the plane $z = 0$ becomes quite appreciable compared with the total homogeneous intensity $I_{\mathrm{tot}}^{(h)}$. However, as is evident from Fig. 8, $I_{\mathrm{tot}}^{(i)}(z)$ decreases very rapidly with $z$ in all cases.[29]

## 5. Conclusion

We have studied the contributions of homogeneous and evanescent waves to near-field diffraction patterns. It is clear from our general analysis and from the example presented in Section 4 that changes in the field for propagation distances much smaller than a wavelength are dominated by the decay of the evanescent contribution. Although we have considered only two-dimensional scalar fields, the analysis can be extended to three-dimensional scalar fields and to vector fields in a straightforward manner.

In the future we plan to examine the exact boundary-value problem and approximate boundary conditions that can be used to model the near field more accurately than the Rayleigh–Sommerfeld or Kirchhoff boundary conditions.

The author thanks Emil Wolf, Brian Cairns, and David G. Fischer for their comments on this paper and Weijian Wang for helpful discussions. This work was supported by the U.S. Army Research Office under the University Research Initiative Program, the National Science Foundation, and the New York State Science and Technology Foundation.

## Appendix A: Total Energy Flux and Total Reactive Energy

In this appendix we discuss the scalar analog of the complex Poynting theorem[30–32] and derive Eqs. (3.9)

of the text for the total energy flux and the total reactive energy.

For a 2-D monochromatic scalar field one can define a complex time-averaged energy flux vector $\mathbf{F}(x, z)$ by the expression

$$\mathbf{F}(x, z) \equiv 2i\omega\alpha U(x, z)\nabla U^*(x, z), \tag{A.1}$$

where $\alpha$ is a real, positive constant and $\nabla = \hat{\mathbf{x}}\partial/\partial x + \hat{\mathbf{z}}\partial/\partial z$, $\hat{\mathbf{x}}$ and $\hat{\mathbf{z}}$ being unit vectors along the positive $x$ and $z$ directions, respectively. Taking the divergence of Eq. (A.1) and using Eq. (2.1), we obtain the relation

$$\nabla \cdot \mathbf{F}(x, z) + 2i\omega\,\mathscr{E}(x, z) = 0, \tag{A.2}$$

$$\mathscr{E}(x, z) \equiv \alpha[k^2|U(x, z)|^2 - |\nabla U(x, z)|^2]. \tag{A.3}$$

Equation (A.2) is exactly of the same form as the complex Poynting theorem in source-free regions. The energy flux vector $\mathbf{F}(x, z)$ is analogous to the complex Poynting vector, and the quantity $\mathscr{E}(x, z)$ is analogous to the difference between the electric and the magnetic energy densities that appears in the complex Poynting theorem.

By integrating Eq. (A.2) over a finite volume $\mathscr{V}$ bounded by a surface $\mathscr{S}$ and applying Gauss' theorem, we can rewrite the equation in the integral form

$$\int_{\mathscr{S}} \mathbf{F}(x, z) \cdot \hat{\mathbf{n}}\,\mathrm{d}S + 2i\omega \int_{\mathscr{V}} \mathscr{E}(x, z)\,\mathrm{d}V = 0, \tag{A.4}$$

where $\hat{\mathbf{n}}$ is the outward unit normal to the volume $\mathscr{V}$ and $\mathrm{d}S$ is an element of surface area. Alternatively, by taking the real (Re) and the imaginary (Im) parts of Eq. (A.4), we have

$$\int_{\mathscr{S}} \mathrm{Re}[\mathbf{F}(x, z) \cdot \hat{\mathbf{n}}]\,\mathrm{d}S = 0, \tag{A.5}$$

$$\int_{\mathscr{S}} \mathrm{Im}[\mathbf{F}(x, z) \cdot \hat{\mathbf{n}}]\,\mathrm{d}S + 2\omega \int_{\mathscr{V}} \mathscr{E}(x, z)\,\mathrm{d}V = 0. \tag{A.6}$$

Equation (A.5) shows that there is no net energy flux through the closed volume, and Eq. (A.6) gives the energy balance for the reactive energy stored in the volume.

From the above considerations we see that the total energy flux and the total reactive energy across any plane $z = \text{const.}$ may be defined by the formulas[33]

$$F_{\mathrm{tot}}^{(h)}(z) \equiv \int_{-\infty}^{\infty} \mathrm{Re}[\mathbf{F}(x, z) \cdot \hat{\mathbf{z}}]\,\mathrm{d}x, \tag{A.7a}$$

$$F_{\mathrm{tot}}^{(i)}(z) \equiv \int_{-\infty}^{\infty} \mathrm{Im}[\mathbf{F}(x, z) \cdot \hat{\mathbf{z}}]\,\mathrm{d}x, \tag{A.7b}$$

respectively. If we now use Eqs. (2.2), (2.3), (A.1), and (A.7), we readily find that $F_{\mathrm{tot}}^{(h)}$ and $F_{\mathrm{tot}}^{(i)}(z)$ may be rewritten in terms of the spectral amplitude function $a(u_x)$ as

$$F_{\mathrm{tot}}^{(h)} = 4\pi\omega\alpha \int_{|u_x|\le 1} (1 - u_x^2)^{1/2}|a(u_x)|^2\,\mathrm{d}u_x, \tag{A.8a}$$

$$F_{\mathrm{tot}}^{(i)}(z) = 4\pi\omega\alpha \int_{|u_x|>1} (u_x^2 - 1)^{1/2}|a(u_x)|^2 \times \exp[-2kz(u_x^2 - 1)^{1/2}]\,\mathrm{d}u_x, \tag{A.8b}$$

which are Eqs. (3.9a) and (3.9b) of the text. We used the superscripts $(h)$ and $(i)$ here because, from the limits of integration in Eqs. (A.8), we see that the total energy flux $F_{\mathrm{tot}}^{(h)}$ depends only upon the homogeneous contribution, and the total reactive energy $F_{\mathrm{tot}}^{(i)}(z)$ depends only upon the evanescent contribution. We also omitted the $z$ argument in $F_{\mathrm{tot}}^{(h)}$ because the total energy flux is independent of $z$.

## References and Notes


1. E. Betzig and J. K. Trautman, "Near-field optics: microscopy, spectroscopy, and surface modification beyond the diffraction limit," Science **257,** 189–195 (1992).
2. U. Dürig, D. W. Pohl, and F. Rohner, "Near-field optical-scanning microscopy," J. Appl. Phys. **59,** 3318–3327 (1986).
3. D. W. Pohl, "Scanning near-field optical microscopy," in *Advances in Optical and Electron Microscopy* (Academic, New York, 1991), Vol. 12, pp. 242–312.
4. E. Betzig, J. K. Trautman, R. Wolfe, E. M. Gyorgy, P. C. Finn, M. H. Kryder, and C.-H. Chang, "Near-field magneto-optics and high-density data storage," Appl. Phys. Lett. **61,** 142–144 (1992).
5. J. E. Harvey, "Fourier treatment of near-field scalar diffraction theory," Am. J. Phys. **47,** 974–980 (1979).
6. G. A. Massey, "Microscopy and pattern generation with scanned evanescent waves," Appl. Opt. **23,** 658–660 (1984).
7. W. H. Carter, "Band-limited angular-spectrum approximation to a scalar dipole field," Opt. Commun. **2,** 142–148 (1970).
8. W. H. Carter, "Band-limited angular-spectrum approximation to a spherical scalar wave field," J. Opt. Soc. Am. **65,** 1054–1058 (1975).
9. See, for example, M. Born and E. Wolf, *Principles of Optics*, 6th ed. (Pergamon, New York, 1980), pp. 560–561, or D. Maystre, "Rigorous vector theories of diffraction gratings," in *Progress in Optics*, E. Wolf, ed. (North-Holland, New York, 1984), Vol. XXI, pp. 1–67.
10. J. W. Goodman, *Introduction to Fourier Optics* (McGraw-Hill, New York, 1968), pp. 48–54.
11. L. Mandel and E. Wolf, *Optical Coherence and Quantum Optics* (Cambridge U. Press, Cambridge, UK, in press), Sec. 3.2.
12. D. C. Bertilone, "The contributions of homogeneous and evanescent plane waves to the scalar optical field: exact diffraction formulae," J. Mod. Opt. **38,** 865–875 (1991).
13. D. C. Bertilone, "Wave theory for a converging spherical incident wave in an infinite-aperture system," J. Mod. Opt. **38,** 1531–1536 (1991).
14. G. C. Sherman, J. J. Stamnes, A. J. Devaney, and É. Lalor, "Contribution of the inhomogeneous waves in angular spectrum representations," Opt. Commun. **8,** 271–274 (1973).
15. G. C. Sherman, J. J. Stamnes, and É. Lalor, "Asymptotic approximations to angular-spectrum representations," J. Math. Phys. **17,** 760–776 (1976).

16. See, for example, A. Papoulis, *Systems and Transformations with Applications in Optics* (McGraw-Hill, New York, 1968), pp. 81–83.
17. J. J. Stamnes, *Waves in Focal Regions* (Hilger, London, 1986), p. 43.
18. D. Slepian, "Some comments on Fourier analysis, uncertainty and modeling," SIAM Rev. **25,** 379–393 (1983).
19. B. R. Frieden, "Evaluation, design and extrapolation methods for optical signals, based on use of the prolate functions," in *Progress in Optics*, E. Wolf, ed. (North-Holland, New York, 1971), Vol. IX, pp. 311–407.
20. G. Toraldo di Francia, "Degrees of freedom of an image," J. Opt. Soc. Am. **59,** 799–804 (1969).
21. E. Wolf and T. Habashy, "Reconstruction of scattering potentials from incomplete data," J. Mod. Opt. **41,** 1679–1685 (1994).
22. A. W. Lohmann, "Three-dimensional properties of wave fields," Optik **51,** 105–117 (1978).
23. G. C. Sherman, "Diffracted wave fields expressible by plane-wave expansions containing only homogeneous waves," J. Opt. Soc. Am. **59,** 697–711 (1969).
24. M. W. Kowarz and E. Wolf, "Conservation laws for partially coherent free fields," J. Opt. Soc. Am. A **10,** 88–94 (1993).
25. M. W. Kowarz, "Conservation laws for free electromagnetic fields," J. Mod. Opt. **42,** 109–115 (1995).
26. M. W. Kowarz, "Energy constraints in optimum apodization problems," Opt. Commun. **110,** 274–278 (1994).
27. E. Wolf and E. W. Marchand, "Comparison of the Kirchhoff and the Rayleigh–Sommerfeld theories of diffraction at an aperture," J. Opt. Soc. Am. **54,** 587–594 (1964).
28. For the case of a circular aperture a comparison of the approximate theories with the exact results may be found in C. J. Bouwkamp, "Theoretical and numerical treatment of diffraction through a circular aperture," IEEE Trans. Antennas Propagat. **AP-18,** 152–176 (1970), and a comparison with experimental results may be found in E. W. Marchand and E. Wolf, "Consistent formulation of Kirchhoff's diffraction theory," J. Opt. Soc. Am. **56,** 1712–1722 (1966). In Bouwkamp's paper the two Rayleigh–Sommerfeld theories are referred to as improved Kirchhoff theories.
29. The decay of the total evanescent intensity $I_{\mathrm{tot}}^{(i)}(z)$ with $z$ is much more rapid for the cases $d = 1\lambda$ and $d = 5\lambda$, shown in Fig. 8. We may explain this behavior by performing an asymptotic expansion of Eq. (4.4b) for large $kz$. One then finds that, when the slit width is an integer number of wavelengths, the first term in the asymptotic expansion vanishes and a higher-order term, which decays more rapidly with $z$, becomes important.
30. H. Levine and J. Schwinger, "On the theory of diffraction by an aperture in an infinite plane screen. I," Phys. Rev. **74,** 958–974 (1948), Eq. (2.24).
31. J. D. Jackson, *Classical Electrodynamics*, 2nd ed. (Wiley, New York, 1975), pp. 241–243.
32. J. A. Stratton, *Electromagnetic Theory* (McGraw-Hill, New York, 1941), pp. 135–137.
33. The electromagnetic analog of these quantities is discussed in G. V. Borgiotti, "Radiation and reactive energy of aperture antennas," IEEE Trans. Antennas Propagat. **AP-11,** 94–95 (1963).